CAPABILITIES OF SATELLITE LASER RANGING SYSTEMS IN NEO OBSERVATIONS

Olli Wilkman, Arttu Raja-Halli, Jyri Näränen, and Niko Kareinen

Finnish Geospatial Research Insitute FGI, Masala, Finland. Email: olli.wilkman@nls.fi

ABSTRACT

Satellite Laser Ranging (SLR) is an established technique for precise orbit determination (POD) of man-made space objects. SLR systems are able to track fast-moving objects in the sky, but require accurate ephemerides for target acquisition. So far, the target objects of SLR have been satellites equipped with purpose-built retro-reflectors. For such objects, the ranging accuracy is on the order of centimeters or better.

In recent years, the interest in applying SLR systems for space debris studies has grown, particularly in Europe. Stations have been equipped with more powerful lasers, and the fast pulse rate of modern lasers allows for statistically significant numbers of ranging pulses in a shorter amount of time. The target selection is, however, still limited to large and bright objects in relatively low orbits, such as spent rocket stages. With such targets, the ranging accuracy is in the same order as the size of the object, as the exact reflection location is not well-defined. With enough observational data, the distribution of ranges can also be used to estimate the size of the object.

Small asteroids pass near the Earth, within the sphere of human satellite operations. With enough advance warning, such close encounters could be tracked with SLR systems. Unfortunately asteroids are challenging targets for laser ranging due to their dark surface. We simulate SLR signal levels from small asteroids, in order to estimate the distance/size relationship of observable NEOs with modern SLR systems. We find that asteroid observations with SLR systems are generally not feasible, due to the small flux of suitable targets close enough to the Earth. However, under favourable conditions

Keywords: satellite laser ranging; NEO.

1. INTRODUCTION

Satellite laser ranging (SLR) is originally a geodetic observation technique, in which distances between ground stations and orbiting satellites are measured accurately from the flight time of laser pulses. In geodetic work, the satellites are equipped with retro-reflectors which return bright and well-defined reflections, allowing range accuracies down to the millimeter level [1]. The precise ranges allow for precise orbit determination for the target satellites. Geodetic satellites are used to measure various time-evolving geodetic parameters, such as the location of the Earth's center of mass. Geodetic SLR observations are performed by a global network of stations, most of them in Europe, Australia and North America.

As laser and detector technology has developed, SLR stations have increased in capability. Modern SLR stations can transmit pulses at kilohertz rates. Combined with sensitive single-photon detectors this allows for the detection of statistically significant numbers of reflections much more quickly.

These developments have also allowed experiments with SLR systems with targets without retro-reflectors, such as space debris [3]. Such targets are much more challenging, as the reflected signal power is many orders of magni-

tudes lower, and the exact reflection point of the returning pulse is ill-defined on the surface of the target object. Still, with targets that are large, bright and near enough, successful observations can be made. With good enough data, estimates can be made of the size, and possibly even the rotational state of the object [7].

In this study, we estimate the capability of existing SLR systems in observing natural objects passing very close to the Earth, mainly near-Earth asteroids in the size scale of 1 meter and larger. Asteroids are very challenging targets for an SLR system, because they are relatively small and dark. Laser ranging systems also require good *a priori* ephemerides for the body, in order to accurately aim the transmitted beam. Such predictions are generally not available ahead of time for small bodies which pass near the Earth.

In Section 2 we describe the methods used in this study. Section 3 gives an overview of the results and Section 4 discusses their implications.

2. METHODS

2.1. Scattering model

As a model for asteroid reflection properties, we use the Lommel-Seeliger scattering model [6], which has the form

$$R(\mu_0, \mu, \alpha) = \frac{1}{4}\omega P(\alpha)\frac{1}{\mu_0 + \mu}, \qquad (1)$$

where ω is the single-scattering albedo and $P(\alpha)$ the single-scattering phase function of the surface, and μ_0 and μ are the direction cosines, i.e. cosines of the angles between the surface normal and the incident and emergent light directions.

In the present work, we only consider monostatic laser ranging and therefore are only concerned with the backscattering direction. This means that $\alpha = 0$ and $\mu_0 = \mu$.

The disk-integrated brightness in the backscattering direction, for a general three-axial ellipsoid with semi-axes a, b and c, is

$$L = \frac{1}{8}\omega F_0 P(0)\pi abcS, \qquad (2)$$

where F_0 is the incident flux on the surface (Watts per square meter), and

$$S = \sqrt{\left(\frac{e_x}{a}\right)^2 + \left(\frac{e_y}{b}\right)^2 + \left(\frac{e_z}{c}\right)^2}, \qquad (3)$$

when $\hat{e} = (e_x, e_y, e_z)$ is the unit vector in the direction of the transmitter and receiver. Here $\pi abcS$ is the cross section area of the ellipsoid projected in the direction $\hat{e}$.

The optical cross-section σ is the area of a diffuse (Lambertian) disk with the same disk-integrated brightness as the target object. By this definition,

$$\sigma = \frac{1}{8}\omega P(0)\pi abcS, \qquad (4)$$

For a sphere with radius r, the optical cross section is

$$\sigma = \frac{1}{8}\omega P(0)\pi r^2 \qquad (5)$$

$$= p\pi r^2 \qquad (6)$$

where $p = \omega P(0)/8$ is the geometric albedo, which by definition is the disk-integrated brightness divided by that of an equal-sized Lambertian disk.

We assume that the target object is completely and uniformly illuminated by the laser beam. This is not strictly true for the largest objects at high altitudes, which leads to a small overestimation of observable target numbers at the large end of the size distribution. However, these objects are so rare that this makes no significant difference to the conclusions.

For a single transmitted laser pulse, expected number of photoelectrons generated in the detector, ϕ, is computed from the radar link equation [1],

$$\phi = \eta_q \left(E_T \frac{\lambda}{hc} \right) \eta_t G_t \sigma \left(\frac{1}{4\pi R^2} \right)^2 A_r \eta_r T_a^2 T_c^2, \tag{7}$$

where η_q is the detector quantum efficiency, E_T is the energy of the laser pulse, λ is the laser wavelength, h the Planck constant, c the speed of light, η_t the efficiency of the transmit optics, G_t the transmitter gain, σ the target's optical cross section, R the slant range to the target, A_r the telescope aperture area, η_r the efficiency of the receive optics, T_a the one-way atmospheric transmission and T_c the one-way transmission of possible cirrus clouds.

2.2. Observability criteria

We define a *significant reflection* as one where at least n_t photoelectrons are produced in the detector. An observation is defined as a rate of at least k significant reflections per second. The values of n_t and k must be chosen, and we choose $n_t = 2$ and $k = 6$.

From Equation 7, we get the expected number of photoelectrons per second, ϕ. We can then model the number of actually received electrons n as Poisson distributed with parameter ϕ. In this case, the probability of a significant reflection is

$$P(n > n_t|\phi) = 1 - e^{-\phi} \sum_{m=0}^{n_t-1} \frac{\phi^m}{m!}. \tag{8}$$

The rate of significant reflections also depends on the laser fire rate f (pulses per second). The probability of exactly m significant reflections per second comes from the binomial distribution,

$$P(m|f,p) = \binom{f}{m} p^m (1-p)^{f-m}, \tag{9}$$

where p is the probability of a significant reflection, from Equation 8.

The probability of at least k significant reflections per second is then

$$P_{\text{detect}}(k|f,p) = 1 - \sum_{m=0}^{k-1} \binom{f}{m} p^m (1-p)^{f-m} \tag{10}$$

The equations above are easily implemented in code, and used to compute the probability of observing a given object.

2.3. Flux of natural objects in Near-Earth space

We compare our observability estimates to a rough estimate of the flux of small bodies in near-Earth space. We use an estimated number of objects impacting the Earth as a baseline [8]. The cumulative number of impactors per year as a function of energy is given as a power law,

$$N = 3.7E^{-0.9}, \tag{11}$$

where E is the kinetic energy in TNT-kiloton equivalents (4.18×10^{12} Joules). This is converted into diameters with numbers used in [8]: a mass-weighed velocity of 20.3 m/s and an average density of 3 g/cm^3.

The distribution is visualized in Figure 1. The flux of impactors with a diameter of 1 m or smaller is of the order of 10/year. For 10 m objects this is of the order 10^{-1}/year and for 100 m of the order 10^{-4}/year.

We estimate the number of objects passing through a spherical volume with radius R_s around the Earth's center by scaling the impact numbers by the area ratio $(R_s/R_{\text{Earth}})^2$. This ignores the focusing effects of the Earth's gravitational field [5], and over-estimates number of objects by a small factor, but is correct within an order of magnitude.

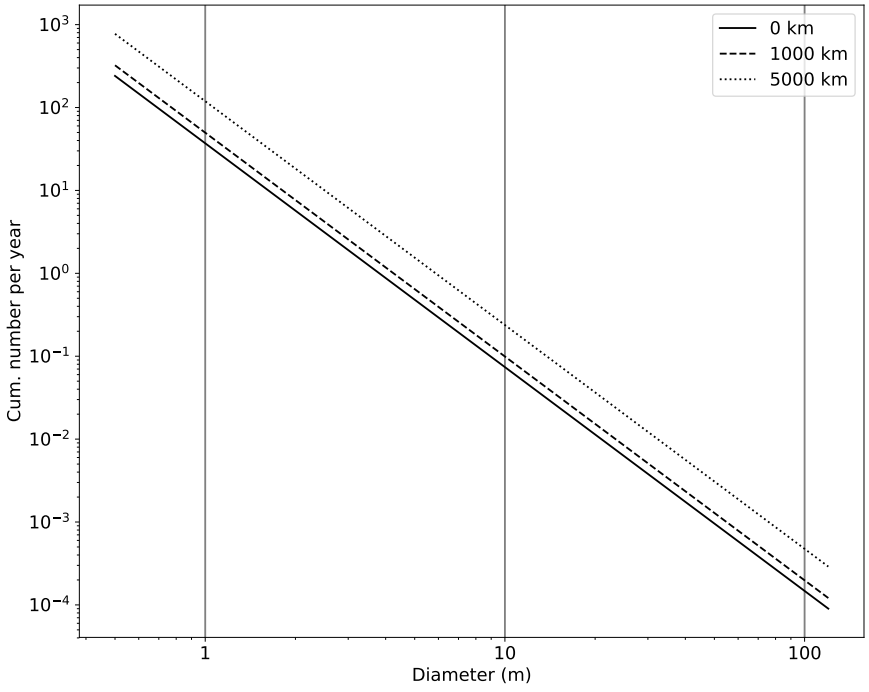

Figure 1. The cumulative number of bodies per year larger than the given diameter, passing through a sphere with a given altitude above the Earth's surface. The solid line shows the number of bodies impacting the Earth, while the dashed and dotted lines show 1000 and 5000 km altitudes.

3. RESULTS

We compute observability statistics using three different SLR setups. The first is a typical modern geodetic SLR system, based on the parameters of the Metsähovi SLR, with a fast 2 kHz laser and 50 cm aperture. The second is a similar system, but with a more powerful laser for space debris observations. The third one is a very powerful laser with a large telescope, loosely based on the the 3.5 m Apache Point Observatory Lunar Laser-ranging Operation (APOLLO). See Table 1 for details.

The other parameters of the radar link equation are the same for all three systems, they are given in Table 2. Atmospheric and cirrus cloud transmittance is computed using formulas from [1]. The station altitude is set to near sea level. These numbers were chosen to represent typical observing conditions.

	Geodetic	Debris	Powerful
Aperture (m^2)	0.188	0.188	2.60
Energy (mJ)	0.40	80	115
Fire rate (Hz)	2000	200	20

Table 1. Parameters of the three simulated laser ranging systems.

	All systems
Transmit optics efficiency η_t	0.93
Receive optics efficiencyη_r	0.82
Transmit gain G	7.37×10^9
Atmospheric transmittance T_a	0.84
Cirrus cloud thickness t	1.3

Table 2. Parameters shared by all three simulated laser ranging systems.

The computations shown below use a zenith angle of 15°. As the zenith angle grows, the signal is attenuated by the atmosphere and the slant range to a target with constant altitude increases. For zenith angles less than 30° the changes are small, but above 45° the number of detectable objects drops rapidly.

Figure 2 shows the detection probability at 1000 km altitude, as a function of target diameter, when the geometric albedo is 0.10. The figure shows that the detection probability decreases from 1 to 0 very rapidly at a certain cut-off size as the target gets smaller. The same general behaviour is seen for all system configurations, zenith angles and geometric albedos. The cut-off size at a given altitude, or vice versa, is therefore a good single number measure for the observability. We define this cut-off as the size where the probability is 50%.

Using the previous cut-off definition, Figure 3 shows the limiting altitude above which observation probability is less than 50%, this time as a function of optical cross section. We highlight three cross section ranges corresponding to spheres of 1 m, 10 m and 100 m diameter, with a geometric albedo range of 0.05 to 0.20 (see Equation 6). Under the curve the probability of detection is ≈ 1 and above it it is ≈ 0.

By combining the altitude vs. cross section relationship shown in Figure 3 with the flux of near-Earth objects shown in Figure 1, we can compute an estimate for the number of observable objects. This is shown in Figure 4. The values shown are the fluxes of objects passing closer than the maximum detectable altitude of the given size. A geometric albedo of 0.10 is assumed in this figure. The figure shows that the laser configuration does not have a large effect on the observable numbers.

4. DISCUSSION

The main conclusion from the simulations is that while modern satellite laser ranging systems can be useful in space debris observations, they are generally not feasible for observations of natural objects passing the Earth. The main limitation is the small flux of large enough target objects. Small, meter-sized objects could be regularly observable, according to the naive numbers estimate of Figure 4. In practice SLR observations require the targets to be already discovered and have accurate ephemeris, which is not likely for the smallest bodies. This limitation will be slightly mitigated in the future by more powerful sky surveys, such as the Large Synoptic Survey Telescope (LSST), which will discover larger volumes of small near-Earth objects.

The most interesting candidates for future laser ranging are the so-called temporarily captured objects (TCO), or “minimoons”, which can

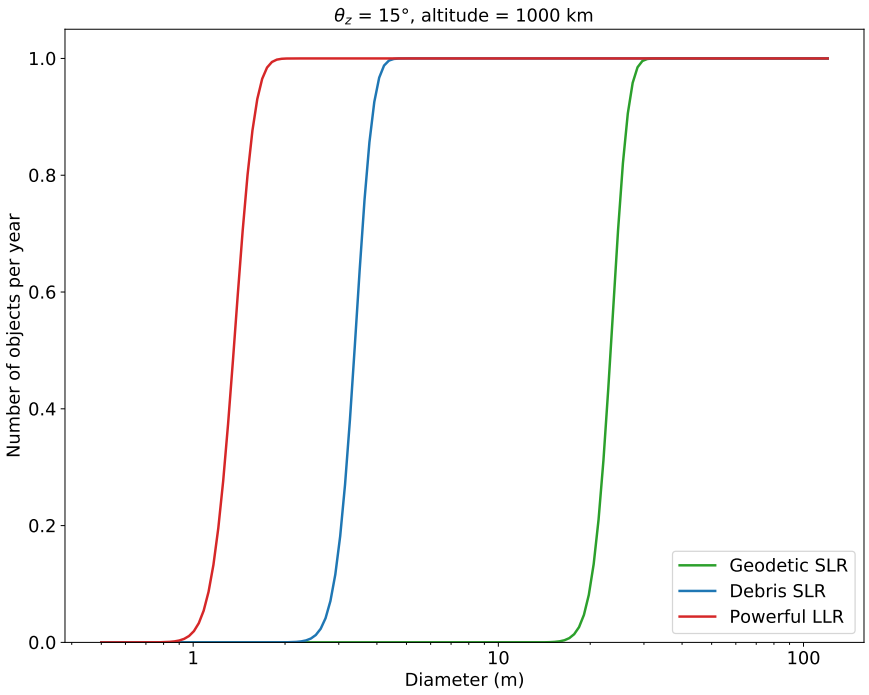

Figure 2. The probability of detection at an altitude of 1000 km and zenith angle of 15° as a function of the object's diameter, when the geometric albedo $p = 0.10$. The three lines correspond to the three laser ranging system configurations (see text).

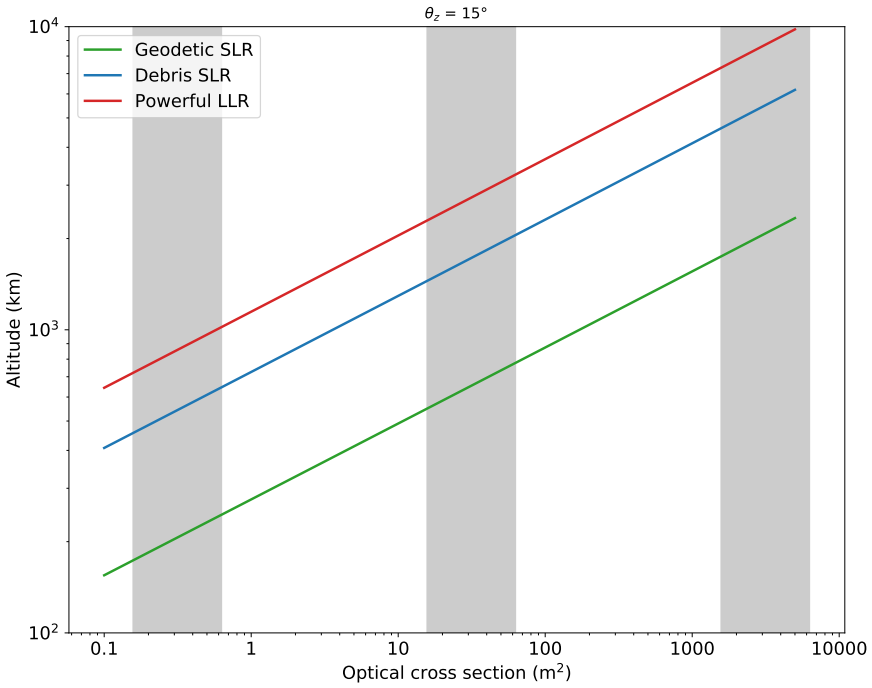

Figure 3. The maximum altitude at which objects of a given optical cross section are observable with a 50% probability. A zenith angle of 15° is assumed. The maximum altitude decreases rapidly for zenith angles greater than 45°. The three curves correspond to the three laser ranging system configurations (see text). The shaded bands correspond to 1 m, 10 m and 100 m diameter spherical objects with a geometric albedo range of 0.05–0.20.

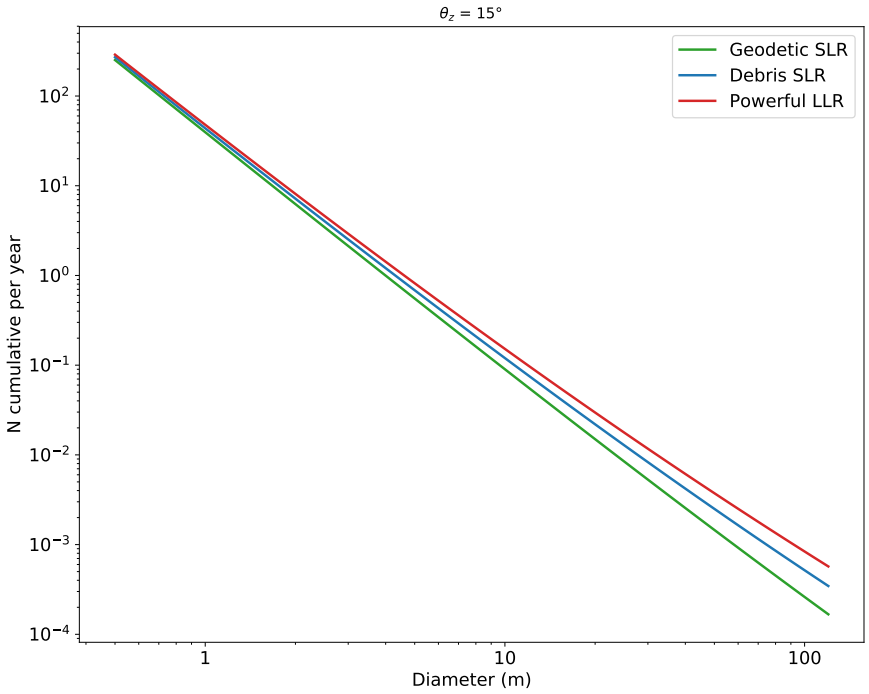

Figure 4. Expected cumulative numbers of observable bodies as a function of optical cross section. On the x axis is the optical cross section; the shaded bands correspond to 1 m, 10 m and 100 m diameter spherical objects with a geometric albedo range of 0.05–0.20. The y axis shows the expected number of objects of a certain cross section or larger, per year, passing closer than the maximum altitude. The numbers do not depend on strongly on the zenith angle, shown here is the 15° case.

linger in the Earth-Moon system on chaotic orbits for a considerable time (several Earth orbits). It is estimated that there is approximately one TCO in the 1–2 meter range at any given time [4], though their average distance is too high for laser ranging [2]. If such objects were to pass close enough to the Earth, they could provide SLR observation opportunities after discovery.

Because of the relatively low energy cost of spacecraft TCOs have also been suggested as targets for low-cost sample-return missions, test cases for impact hazard mitigation techniques, and even as first steps in space resource exploitation [4]. Sending a small spacecraft to attach itself onto the asteroid would allow both active (radio) and passive tracking methods (laser reflectors) to be used. A simple radio beacon would provide much more practical value for tracking, but also depends on the spacecraft systems for power and control. A retro-reflector is a very low-cost and light addition, while being completely passive and potentially observable with Lunar laser ranging systems. A retro-reflector also provides significantly higher ranging precision, which can be an advantage when studying the chaotic dynamics of a TCO.

ACKNOWLEDGEMENTS

This work has been supported by the Academy of Finland (project number 298139), as well as Finland's Scientific Advisory Board For Defence (MATINE).

REFERENCES

1. J. J. Degnan. Millimeter accuracy satellite laser ranging: A review. In D. E. Smith and D. L. Turcotte, editors, *Contributions of Space Geodesy to Geodynamics: Technology*, volume 25. AGU Geodynamics Series, 1993.

2. G. Fedorets, M. Granvik, and R. Jedicke. Orbit and size distributions for asteroids temporarily captured by the earth-moon system. *Icarus*, 285:83–94, 2017.

3. T. Flohrer, B. Jilete, H. Krag, Q. Funke, V. Braun, and A. Mancas. ESA activities on laser ranging to non-cooperative targets. In *The 2016 International Workshop on Laser Ranging, Potsdam, Germany*, October 9–14, 2016.

4. R. Jedicke, B. T. Bolin, W. F. Bottke, M. Chyba, G. Fedorets, M. Granvik, L. Jones, and H. Urrutxua. Earth's minimoons: Opportunities for science and technology. *Front. Astron. Space Sci.*, 5(13), 2018.

5. J. Jones and L. M. G. Poole. Gravitational focusing and shielding of meteoroid streams. *Monthly Notices of the Royal Astronomical Society*, 375:925–930, Mar. 2007.

6. K. Muinonen, O. Wilkman, A. Cellino, X. Wang, and Y. Wang. Asteroid lightcurve inversion with Lommel-Seeliger ellipsoids. *Planetary and Space Science*, 118:227–241, 2015.

7. O. Wilkman. Ray-tracer for modeling interactions of light with space objects. In *Advanced Maui Optical and Space Surveillance Technologies Conference*, 2018.

8. M. Zolensky, P. Bland, P. Brown, and I. Halliday. Flux of extraterrestial materials. In D. S. Lauretta and H. Y. McSween, editors, *Meteorites and the Early Solar System II*, pages 869–888. University of Arizona Press, Tucson, 2006.